Optica Applicata, Vol. XXXIV, No. 4, 2004

Fourier transform holographic storage

ANDRZEJ ANDRUCHÓW

Institute of Physics, Wrocław University of Technology, Wybrzeże Wyspiańskiego 27,
50-370 Wrocław, Poland

Holographic optical elements for Fourier transform (HOE-FT) used in the optical memory system are considered in this paper. The determination of the optimal page composer capacity allows for the appropriate choice of the diameter of HOE-FT as well as the size of a hologram recorded in the fotorefractive crystal $LiNbO_3$:Fe, with the help of two different wavelengths of the laser light beam. When the interfering field is recorded in the HOE-FT structures, properties of the recorded spectrum are established. The proper choice of the phase function coefficients allows aberration to be corrected on the basis of spotdiagrams obtained.

Keywords: optical system, aberration, spotdiagram.

1. Introduction

The holographic optical elements (HOE) have been considered by many authors [1]–[8]. They are lighter and more compact and can be manufactured easily and quickly compared to conventional lenses, hence the attempt of using them in the optical memory system (OMS). Applying two different wavelengths of light at the same time during the recording of holograms in the OMS makes the repeated read-out of recorded information possible avoiding of use of the fixing techniques [9]–[12]. The system analysed, which is a part of an OMS, consists of an object in the form of page composer (SLM), a holographic lens for HOE-FT and crystal as the information recording medium. The determination of the relationship between these optical elements by analysing the tracking of the principal and marginal rays [13] allows for the optimal choice of the focal length, diameter of the HOE-FT and page composer capacity as well as the size of the hologram that determinates the number of sectors into which the recording material is divided when the spatial multiplexing technique is applied.

The phase function of HOE-FT [1]–[3] given in the form of the recorded interfering pattern determines the page composer information transform into the adequately focused spectrum in the crystal. This paper deals with the research on aberration correction and phase function optimization of the HOE by means of the OSLO Light 6.04 programme.

2. Holographic Fourier transform

The plane wave goes from the source of light situated in the infinity and illuminates the data page composer (SLM) – Fig. 1. The diffracted waves are transformed through the HOE-FT to its back focal plane, where the spectrum of the object is created and recorded in the crystal in the form of a hologram. The page composer, which is the data bit mask, consists of the square (pixels) elements, whose transmittance of amplitude is $t = 0$ or $t = 1$ depending on whether logical one or zero is printed. Each of the cells with transmittance of amplitude $t = 1$ equally diffracts the incident light. The number of all page composer cells determines its capacity. When the cell is small, then the page composer capacity is bigger and the size of hologram becomes magnified. This, however, limits the number of sectors in the storing medium, in the case of application of spatial multiplexing technique. An increase of the focal length of HOE-FT as well as the diffraction angle causes enlargement of the hologram size which is connected with reduction of the cell size of SLM – Fig. 2.

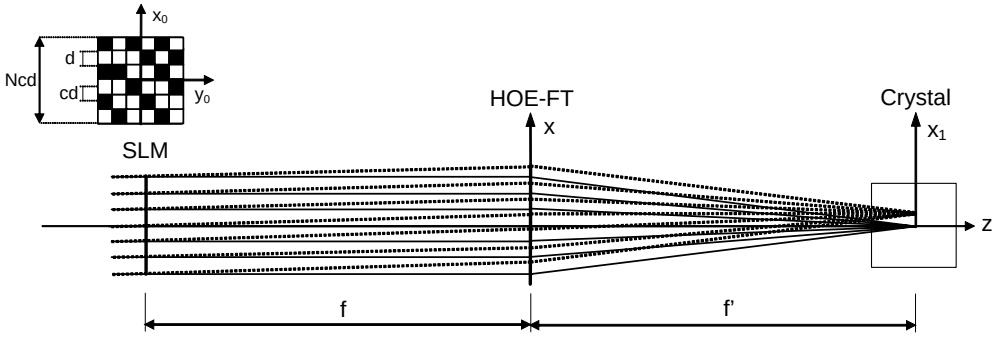

Fig. 1. Ray-tracing in the system of hologram recording.

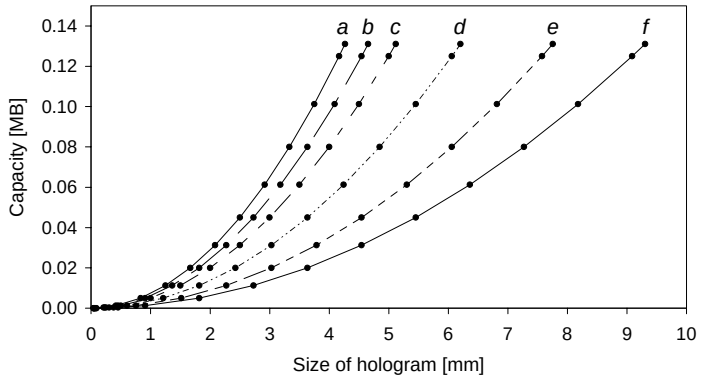

Fig. 2. Capacity of SLM as a function of hologram size for different values of the focal length: 55 mm (*a*), 60 mm (*b*), 66 mm (*c*), 80 mm (*d*), 100 mm (*e*) and 120 mm (*f*).

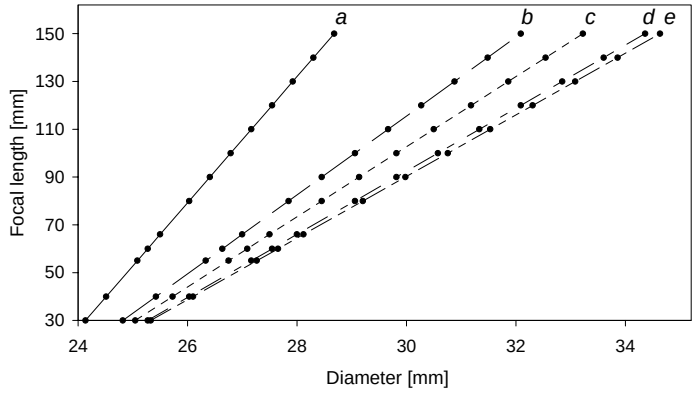

Fig. 3. Focal length as a function of diameter of HOE-FT, for a different number of cells of the SLM: 500 (*a*), 800 (*b*), 900 (*c*), 1000 (*d*), 1024 (*e*).

The diameter of the HOE-FT allowing the diffracted wave imaging on object structures at angles α_x and α_y to suitable spectrum, the coordinates of which are in the Fourier plane ($x_f = f\sin(\alpha_x) = f\lambda_1/d_x$ and $y_f = f\sin(\alpha_y) = f\lambda_1/d_y$), is described by the following formula:

$$S = 2\frac{\lambda_1 f}{d} + Ndc \tag{1}$$

where N, d, c are the SLM parameters describing the number of its cells in one side, the length of pixel side and the ratio of the centre spacing to the bit length. Figure 3 illustrates the dependence between diameter S and different values of focal length. Each of the curves was drawn for different values of N. If parameters N and f decrease, the diameter S becomes smaller.

3. Holographic element phase function

The wave of light transmitted through the structure of data page composer with the phase $\phi_{\text{in}}(x;\ \alpha)$ is transformed by HOE-FT described by the phase function $\phi_h(x)$ to the Fourier plane, where the desired light wave has the phase $\phi_d(x;\ \alpha)$. On the basis of papers [1]–[3], the phase function can by presented in one-dimensional form

$$\phi_h(x) = -\frac{\int w(\theta)p(x;\theta)\phi_H(x;\theta)\,\mathrm{d}\theta}{\int w(\theta)p(x;\theta)\,\mathrm{d}\theta} \tag{2}$$

where: $w(\theta)$, $p(x;\ \theta)$ are the weight and pupil functions having the values from the range [0, 1] and $\phi_H(x;\ \theta) = \phi_d(x;\ \theta) - \phi_{\text{in}}(x;\ \theta)$.

Considering the range of diffracted angle variability on the page composer cells from $\theta_1(x) = -\sin^{-1}(\lambda/d)$ to $\theta_2(x) = \sin^{-1}(\lambda/d)$, which are equal to direction cosines reduces the formula to the form:

$$\phi_h(x) = -\frac{\int_{\theta_1(x)}^{\theta_2(x)} w(\theta)\left[\phi_d(x;\theta) - \phi_{\text{in}}(x;\theta)\right] \mathrm{d}\theta}{\int_{\theta_1(x)}^{\theta_2(x)} w(\theta)\,\mathrm{d}\theta}. \tag{3}$$

Writing down the dependence described by formula (3), taking into account

$$\phi_d(x;\theta_x) = \frac{2\pi}{\lambda_c}\left[-\sqrt{\left(f\sin(\theta_x) - x\right)^2 + f^2}\right],$$

$$\phi_{in}(x;\theta_x) = \frac{2\pi}{\lambda_c}\left[x\sin(\theta_x)\right],$$

$$w(\theta_x) = \cos(\theta_x),$$

we obtain

$$\phi_h(x) = \frac{\frac{2\pi}{\lambda_1}\int_{\theta_1(x)}^{\theta_2(x)} \cos(\theta_x)\left[\sqrt{\left(f\sin(\theta_x) - x\right)^2 + f^2} + x\sin(\theta_x)\right]\mathrm{d}\theta}{\int_{\theta_1(x)}^{\theta_2(x)} \cos(\theta_x)\,\mathrm{d}\theta}. \tag{4}$$

Integrating the expression described by formula (4) we have:

$$\begin{aligned}\phi_h(x) = \frac{2\pi}{\lambda_c}\frac{1}{2fK}\Bigg\{ & f^2 \ln\left(\frac{\sqrt{\left(f\sin(\theta_1) - x\right)^2 + f^2} - f\sin(\theta_1) + x}{\sqrt{\left(f\sin(\theta_2) - x\right)^2 + f^2} - f\sin(\theta_2) + x}\right) \\ & - \left(x - f\sin(\theta_2)\right)\sqrt{\left(f\sin(\theta_2) - x\right)^2 + f^2} \\ & - \left(f\sin(\theta_1) - x\right)\sqrt{\left(f\sin(\theta_1) - x\right)^2 + f^2} + \left[fx\left(\sin(\theta_2) + \sin(\theta_1)\right)K\right]\Bigg\}\end{aligned} \tag{5}$$

where $K = \sin(\theta_2) - \sin(\theta_1)$. In this kind of expression it is difficult to say something about coefficients standing at appropriate powers of x, which provide information about HOE-FT properties. We will obtain more information if the square roots and the expression under logarithm are expanded in the Taylor series for the variable x, simultaneously introducing two-dimensional notation [1] of the phase function for the same values of field angle in x, y plane

$$\phi_h(x, y) = \frac{2\pi}{\lambda_1}\left[\left(x^4 + y^4\right)a_{44} + \left(x^2 + y^2\right)a_{22} + (x + y)a_{11} + a_{00}\right], \tag{6}$$

and

$$a_{00} = \frac{f}{K}\left\{\ln\left[\sin(\theta_2)\sqrt{\left(\sin(\theta_1)\right)^2 + 1} - \sin(\theta_1)\sqrt{\left(\sin(\theta_2)\right)^2 + 1}\right]\right.$$

$$\left. + \sqrt{\left(\sin(\theta_2)\right)^2 + 1}\sqrt{\left(\sin(\theta_1)\right)^2 + 1} - \sin(\theta_2)\sin(\theta_1)\right\}$$

$$+ \frac{3f\left[\left(\sin(\theta_2)\right)^3 - \left(\sin(\theta_1)\right)^3\right]}{PK} + \frac{f\left[\left(\sin(\theta_2)\right)^7 - \left(\sin(\theta_1)\right)^7\right]}{PK}$$

$$+ \frac{3f\left[\left(\sin(\theta_2)\right)^5 - \left(\sin(\theta_1)\right)^5\right]}{PK} + \frac{f}{P},$$

$$a_{11} = \frac{1}{K}\left[\frac{\left(\sin(\theta_1)\right)^2 + 1}{\sqrt{\left(\sin(\theta_1)\right)^2 + 1}} - \frac{\left(\sin(\theta_2)\right)^2 + 1}{\sqrt{\left(\sin(\theta_2)\right)^2 + 1}}\right],$$

$$a_{22} = \frac{5\left[\left(\sin(\theta_2)\right)^2 - \left(\sin(\theta_1)\right)^2\right]}{4fPK} + \frac{3}{4fP} - \frac{1}{4fS} + \frac{\left(\sin(\theta_2)\right)^5 - \left(\sin(\theta_1)\right)^5}{2fPK},$$

$$a_{44} = -\frac{1}{4f^3P}$$

where: $S = [(\sin(\theta_1))^2 + 1]^{3/2}$ and $P = [(\sin(\theta_1))^2 + 1]^{5/2}$. The interfering field described by formula (6) permits the waves diffracted on the object to be converted into the suitable spectrum. The quality of this imaging is determined by the coefficients standing at appropriate power of x and y. The focusing properties are described by the coefficient a_{22} standing at the second power of x and y. The wave of light is focused exactly in the focal plane of the HOE-FT when the factor $a_{22} = 1/(2f)$, which is an equivalent of the situation when rays of the light go very close to the optical axis. Outside the focal plane there occurs over- or underfocusing causing the energy dissipation and simultaneously increasing spherical longitudinal and transversal aberration. In this case, it is necessary for the focal plane to be shifted to the area of the best imaging, taking into account the focal length resulting from the place where the beams of the light rays going near the optical axis intersect.

4. Optical memory system

The light beam of wavelength $\lambda_1 = 852.11$ nm emitted from the diode laser is expanded by the collimator after being reflected from the mirror, then divided by the beam splitter into two reference and object beams – Fig. 4. In each path of beam propagation, there are two acoustooptic deflectors used in the process of addressing to the selected sector or particular crystal location. Transformed by the HOE-FT amplitude and phase modulated by the data page composer wave light interferes with the reference beam in the volume of the recording material (crystal $LiNbO_3$:Fe) in the presence of the light beam of wavelength $\lambda_2 = 488$ nm emitted from the argon laser. This form of storing information by means of two beams of laser light with different wavelength of light λ_1, λ_2 applied at the same time, allows multiple read-outs of stored hologram [9]–[12]. The space charge field, which modulates through the electrooptic Pockels effect the

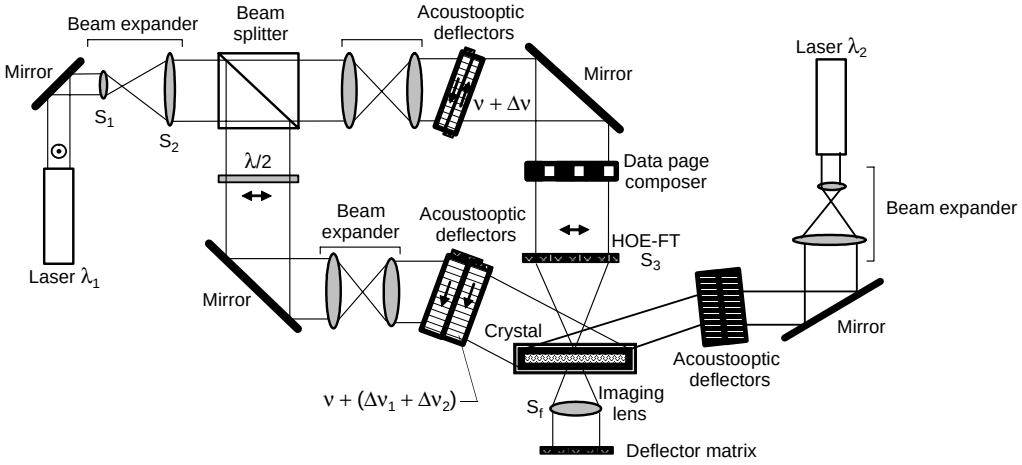

Fig. 4. Ray-tracing in the system of holographic memory.

refraction index of the crystal medium, results from the charge separation under the influence of waves λ_1, λ_2, which have different energy. In this system, a 23×23 mm^2 nematic liquid crystal page composer was used. The size of its cell is 0.0225×0.0225 mm^2, but the range of diffracted angles on its structure changes from $\theta_1 = -2.17°$ to $\theta_2 = 2.17°$. The capacity of the SLM, the diameter and the focal length of HOE-FT are 0.125 MB, 24 mm, 66 mm, respectively. These parameters allow the hologram size of 5 mm to be calculated. That is why, when using a crystal of the size about 15×15×15 mm, we divide it into three sectors using the spatial multiplexing technique. With the help of the imaging lens, information read-out is made on the semiconductor matrix array consisting of the same number of cells as that of the page composer. When using the HOE-FT in the OMS it is necessary to apply the same wavelength of light which was used during the recording process. Hence the limitation in using the wavelength multiplexing technique which allows a bigger capacity of the memory to be obtained compared to the angle multiplexing technique used in this configuration.

5. Results

Based on the data presented here the coefficients of the polynomial phase function has been calculated for the non-corrected HOE-FT, as given in Tab. 1. Then spotdiagrams were obtained, in which the focus plane was shifted at 0.056938 mm – see Fig. 5. For the diffracted angles analysed, an asymmetry in the displacement of energy, suggesting the presence of the coma, can be seen. The focus shift caused by over- and underfocusing increases the transverse spherical aberration influencing the change in the displacement of energy in the spot. One can also notice in the spotdiagrams that the size and shape of the spot on the optical axis is changed as the field angle increases. For its three values we can obtain the diagrams of the point spread function – Fig. 6.

T a b l e 1. Calculated values of the phase function coefficients for the non-corrected HOE-FT.

Coefficients of the polynomial phase function	a_{00}	a_{11}	a_{22}	a_{33}	a_{44}
Calculated values	–1308.77	0	0.00757032	0	-4.332345×10^{-7}

For zero spatial frequency a characteristic peak connected with the maximal intensity of light in the focusing area of light waves which are not diffracted on the object can be observed. For the two remaining field angles, considerable decrements in the amount of energy in the broadening areas of the image, compared to the intensity obtained for zero spatial frequency, can be seen. Comparing the shape of the spectrum for the waves diffracted on the object with spotdiagrams, we notice reciprocal similarity in each of the cases. The asymmetry in the distribution of energy in the spot

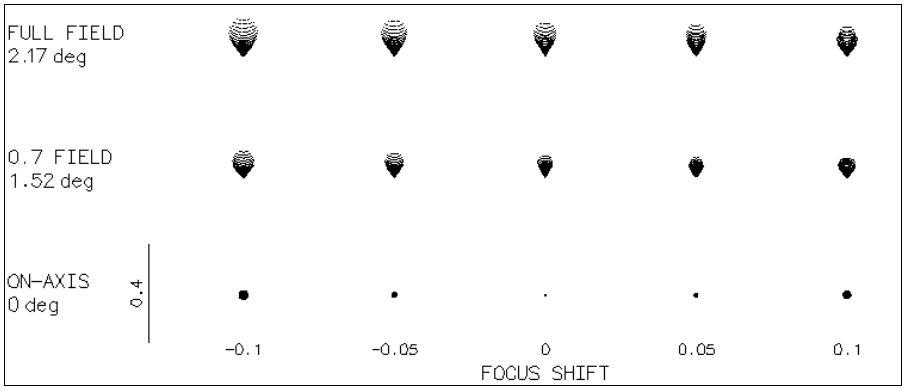

Fig. 5. Spotdiagrams for different field angles, before optimization procedure of HOE-FT.

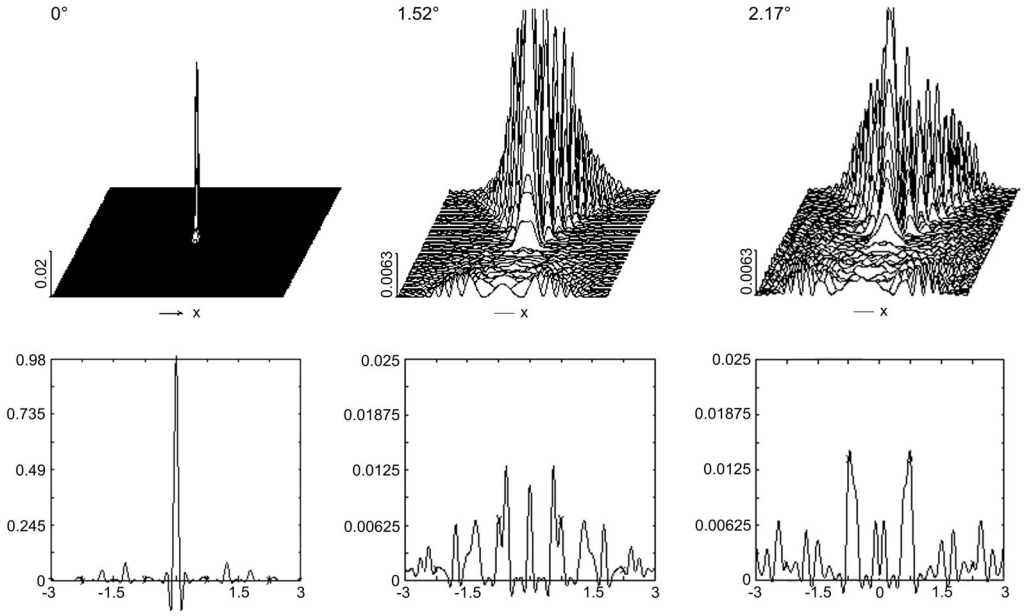

Fig. 6. Point spread function for different field angles before optimization procedure of HOE-FT.

indicates aberration. Through its correction we modify the shape of the spectrum tending to obtain symmetrical distribution of energy in the spot for different values of the field angle. The measure of astigmatism is the distance between the longitudinal and transversal focuses, and through their centres curves have been drawn for different values of the pupil size – Fig. 7**a**.

The reason for the departure from linear character of these curves is simultaneous presence of the field curvature. The size of the spot on the axis is described by the size of the transversal spherical aberration, and the distance of the optical axis intersection

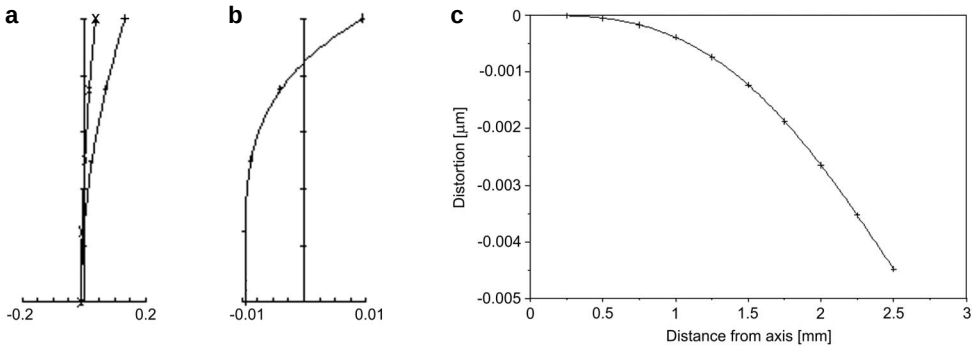

Fig. 7. Diagrams of the aberrations: **a** – astigmatism (in mm), **b** – longitudinal spherical aberration (in mm), **c** – distortion.

by the light rays behind or in front of Fourier plane describes spherical longitudinal aberration – Fig. 7**b**. The dependence of distortion in the function of the field angle, is shown in Fig. 7**c**. After the optimization procedure the obtained values of coefficients included in the phase function (see Tab. 2), differ from those in Tab. 1.

Shifting the Fourier plane of value –0.2 mm resulted in the spotdiagrams shown in Fig. 8. Comparing them with the previous results obtained in the case where there was no correction, it is seen that obtaining symmetrical distribution of energy in the

T a b l e 2. Calculated values of the phase function coefficients for the corrected HOE-FT.

Coefficients of the polynomial phase function	a_{00}	a_{11}	a_{22}	a_{33}	a_{44}
Calculated values	–1308.77	1×10^{-7}	0.00757032	-1×10^{-8}	-1×10^{-8}

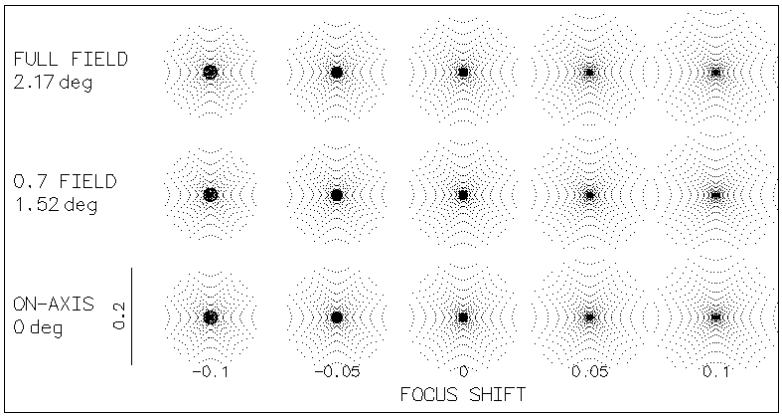

Fig. 8. Spotdiagrams for different field angles for the corrected HOE-FT.

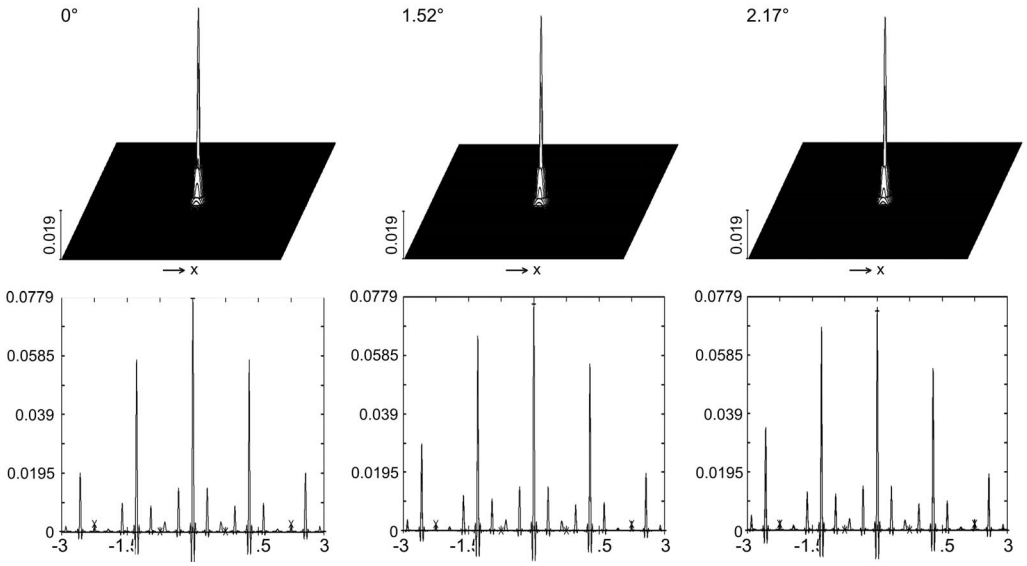

Fig. 9. Point spread function for different field angles after optimization procedure of HOE-FT.

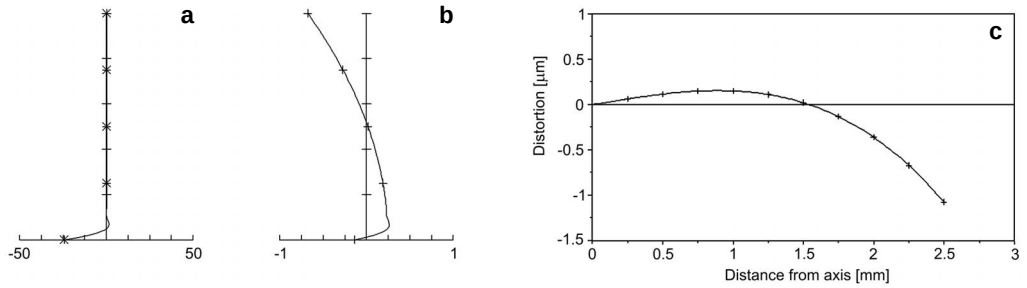

Fig. 10. Diagrams of the aberrations after optimization procedure of HOE-FT: **a** – astigmatism (in mm), **b** – longitudinal spherical aberration (in mm), **c** – distortion.

spot for beams diffracted on an object is connected with increasing the spot size for the zero spatial frequency.

For this reason, the value of spherical transversal aberration increases to 52 µm. The distribution of the point spread function (see Fig. 9) differs from that shown in Fig. 6. In the spectrum for the zero spatial frequency, increasing the value of transversal spherical aberration caused the distribution of energy over a bigger area and decreased intensity. Writing down this kind of distributed spectrum in the form of hologram we do not have to use the phase mask. The aim is to obtain equal spectrum distribution advantageous for the holographic information recording. In the spectrum areas, where the intensity attains almost 1, the dynamic range of material is overflown [14].

Numerically defined coefficients in the Tab. 2 permit the coma, astigmatism and field curvature correction at cost of increasing the longitudinal and transverse spherical aberration as well as distortion Fig. 10.

6. Conclusions

In this paper, the necessity of using HOE-FT in the OMS has been shown, despite the fact that application of the wavelength multiplexing technique to OMS is impossible. Proper matching of the coefficients of polynomial phase function enables aberration correction and influences spectrum recording in the form of holograms making it more advantageous and does not require usage of phase mask. A wider analysis of the problem may concern taking into account the thickness of the HOE-FT and its refraction index, which has not been considered in this paper. Nevertheless, it should not be forgotten that strong diffraction effects taking place at edges of the data page composer cells can cause an increase of the field angle and therefore influence the increasing of HOE-FT diameter *S* as well as the hologram size.

References

[1] HASMAN E., FRIESEM A.A., J. Opt. Soc. Am. A. **6** (1989), 62.
[2] CEDERQUIST J.N., FIENUP J.R., J. Opt. Soc. Am. A. **4** (1987), 699.
[3] GOTO K., TERASAWA A., J. Opt. Soc. Am. A. **7** (1990), 2109.
[4] ONO Y., NISHIDA N., J. Opt. Soc. Am. A. **3** (1986), 139.
[5] AMITAI Y. FRIESEM A.A., J. Opt. Soc. Am. A. **5** (1988), 702.
[6] JAGOSZEWSKI E., ANDRUCHÓW A., Opt. Appl. **34** (2004), 63.
[7] JAGOSZEWSKI E., Optik **69** (1985), 85.
[8] REINHORN S., GORODEISKY S., FRIESEM A.A., AMITAI Y., Opt. Lett. **20** (1995), 495.
[9] ASHLEY J., BERNAL M.P., BURR G.W., COUFAL H., GUENTHER H., HOFFNAGLE J.A., JEFFERSON C.M., MARCUS B., MACFARLANE R.M., SHELBY R.M., SINCERBOX G.T., IBM J. Res. Develop. **44** (2000), 341.
[10] ADIBI A., BUSE K., PSALTIS D., Phys. Rev. A. **63** (2001), 63.
[11] BUSE K., ADIBI A., PSALTIS D., J. Opt. A: Pure Appl. Opt. **1** (1999), 237.
[12] LIU Y., KITAMURA K., TAKEKAWA S., RAVI G., NAKAMURA M., HATANO H., YAMAJI T., Appl. Phys. Lett. **81** (2002), 2686.
[13] VANDER LUGT A., Appl. Opt. **12** (1973), 1675.
[14] ANDRUCHÓW A., *SPIE material from conference Wilga (2004)* – in press.

Received August 2, 2004